ISSN: 0369-8963
PERIODICO di MINERALOGIA Volume 91, No. 3, 2022

# Prediction of Suitable Piston Bowl Chamber for 2,5-Dimethyl Furan (Dmf) Direct Injection on Ci Engine

**M. VELLIANGIRI.[1], G. SURESHKANNAN [2], M. KARTHIKEYAN[3], K. KARTHIK [4]**

*[1, 3, 4] Assistant Professors Department of Mechanical Engineering*

*[2]Associate Professors Department of Mechanical Engineering*

*Coimbatore Institute of Technology- Tamilnadu- INDIA*

## Abstract

*2,5-Dimethyl Furan (DMF) direct injection in compression ignition engine simulation and experimental research article focused on selecting one of the three swirl ratio piston bowls that predicted low ignition delay and was compared to the other two chosen bowls for better combustion. A pump capable of pumping 400 to 1200 bar pressure was set and used for the injection pressure. With a constant compression ratio of 18.54:1, and selected three different swirl ratio piston bowls with the appropriate parameters for comparison. Predicted low ignition delay for an MDF high compression direct injection (HCDI) engine by selecting three different swirl ratio piston bowls. CA, HRR with CA and SFC, NOx, ID, and PM emissions werwere e predicted and compared with variable injection pressure in the in-cylinder pressure (ICP). Low ignition delay is achieved by selecting one of three combustion chambers based on EGR mode (with or without), which ranging % to 15%. Testing confirmed that the performance of a chosen combustion chamber bowl (A) was better than the other two chambers.*

*Keywords*: *Combustion bowl chamber selection, Heat Release Rate, Ignition delay, High compression Ignition, Variable Injection Pressure, Swirl Ratio, DMF Fuelled HCI Engine*

## Introduction

High compression Ignition (HCI) engine research is difficult due to strict emission regulations, such as CO2 and other emissions. Another critical focus on the unpredictability of fossil fuel reserves reinforces the need to continue developing high-efficiency and highly required better combustion engines. Furthermore, renewable energy sources such as bio-fuel create fuel [1]. Greenhouse gas emissions (CO2), NOx emissions, and particle matter (PM) emissions are highly significant emission parameters that must be reduced to near-zero levels. The shape of the combustion bowl chamber is essential for controlling the combustion process, increasing the heat release rate, and improving the emission characteristics of (CI) engines. As a result, the optimisation process for predicting the combustion bowl parameter for HCDI engines is required. Suitable bowl modifications are needed to meet emission standards and acceptable engine performance [2][3]. Previous research articles suggested that the task of direct DMF injection in CI engines was challenging. As a result, one best combustion chamber must be chosen for the ratio to the piston bowl chambers required for combustion [2][1]. Specific Fuel Consumption (SFC), Nitrogen Oxides (NOx), Particulate Matter (PM), and Ignition Delay (ID) are all important DMF -powered High Compression Ignition (HCI) engines. The simulation results were various injection pressures, EGR, and swirl ratios. Previous research suggested the swirl ratio and heat release rate [1][4]. Critical parameters were plotted against various injection pressures and compared in three different combustion chambers and C. Based on

 https://doi.org/10.37896/pd91.3/91329

significant parameter comparisons; one suitable chamber was an enclosure for better combustion and low emission [5][2]. Piston bowl Chamber (A) was selected and built based on the parameters provided to compare the ID of the three chambers. According to the authors, ID is the most crucial parameter when compared to other parameters [6][3][3].

## Methodology And Experimental Setup

This combustion simulation is separated into two significant phases and deals with creating three different piston bowls. Piston bowl swirl ratios vary from 2.5 to 2.9 and 3.1, with a compression ratio of 17.5:1 for diesel fuel DI engines. The second phase is to create three piston swirl ratios varying from 2.3, 2.9 and 3.1 with a constant compression ratio 18.54:1 for the MDF HCI engine. The significant challenges in creating and selecting of one of better among the three are shown in Figures, and 2.3.[2]

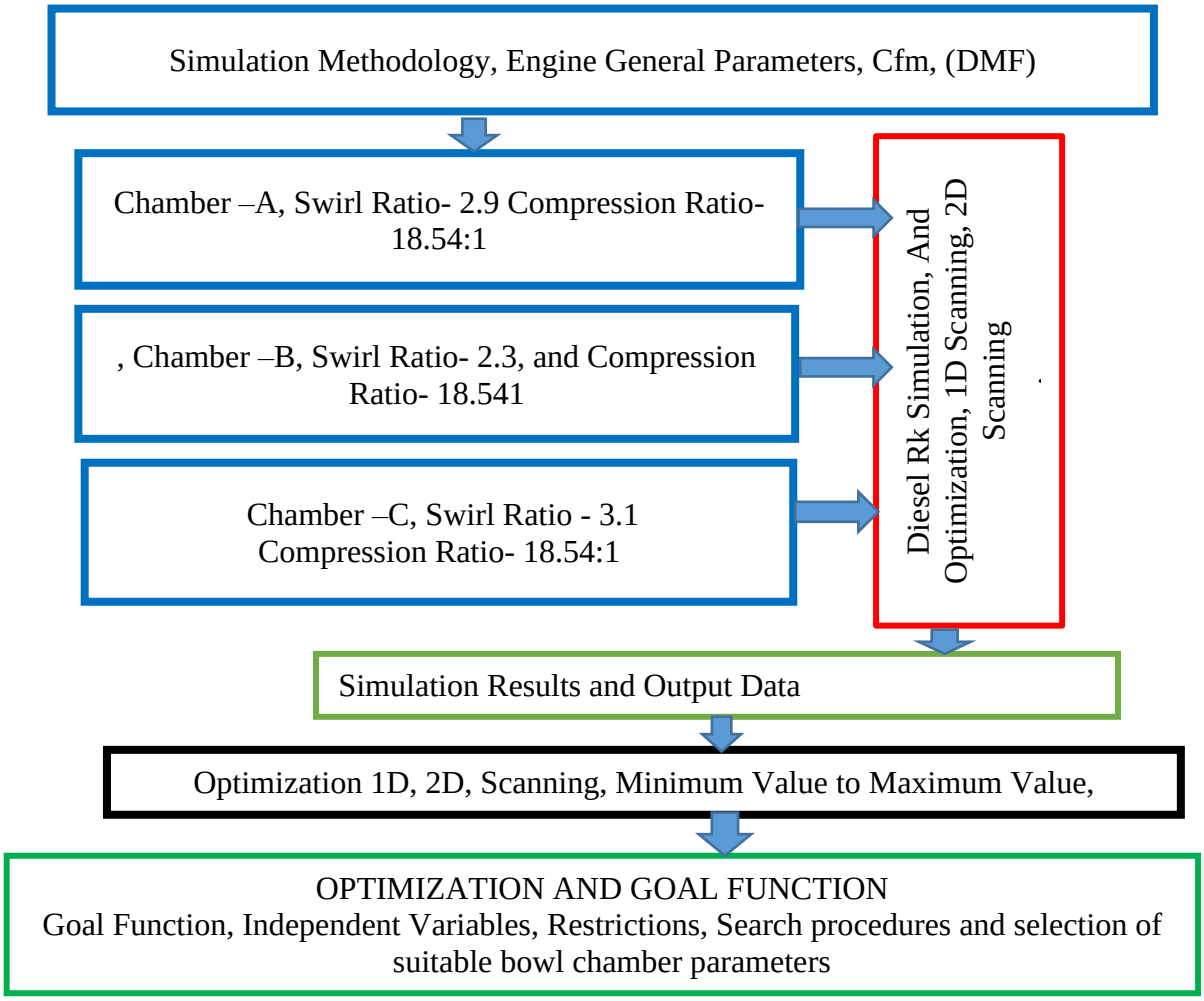


Figure 2.1Diesel RK simulation methodology for DMF


https://doi.org/10.37896/pd91.3/91329

ISSN: 0369-8963
PERIODICO di MINERALOGIA Volume 91, No. 3, 2022

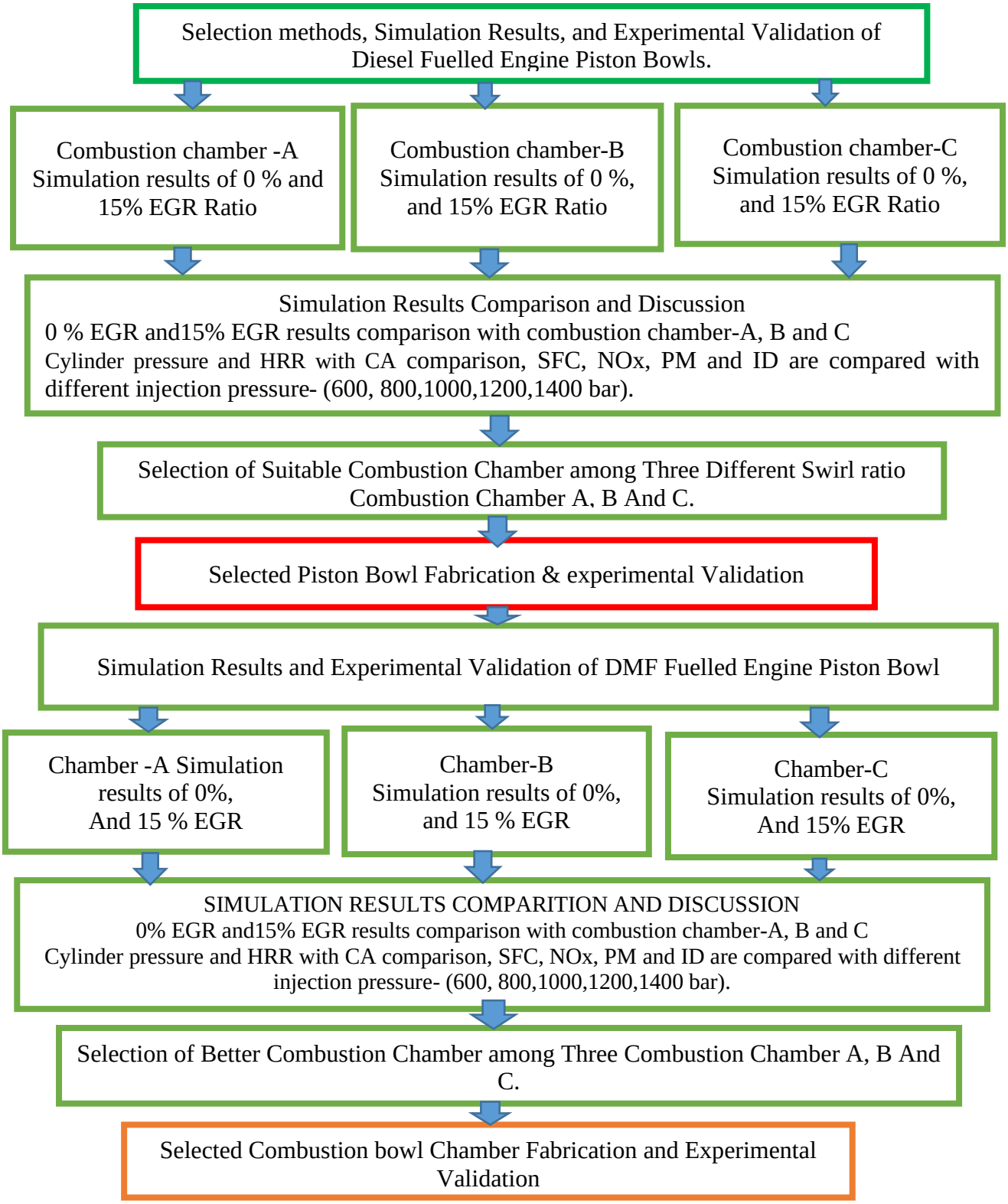


.

Figure 2.2 Simulation Results and Experimental Validation of Diesel Fuelled Engine Piston Bowls

 https://doi.org/10.37896/pd91.3/91329

ISSN: 0369-8963
PERIODICO di MINERALOGIA Volume 91, No. 3, 2022

The most significance of piston bowl parameters namely CR, SR, EGR, injection timing (IT) and injection pressure (INJP) focused to improve efficiency and reduce the emission. Optimum points for piston bowl parameters and achieve the combustion based on the simulation[4].

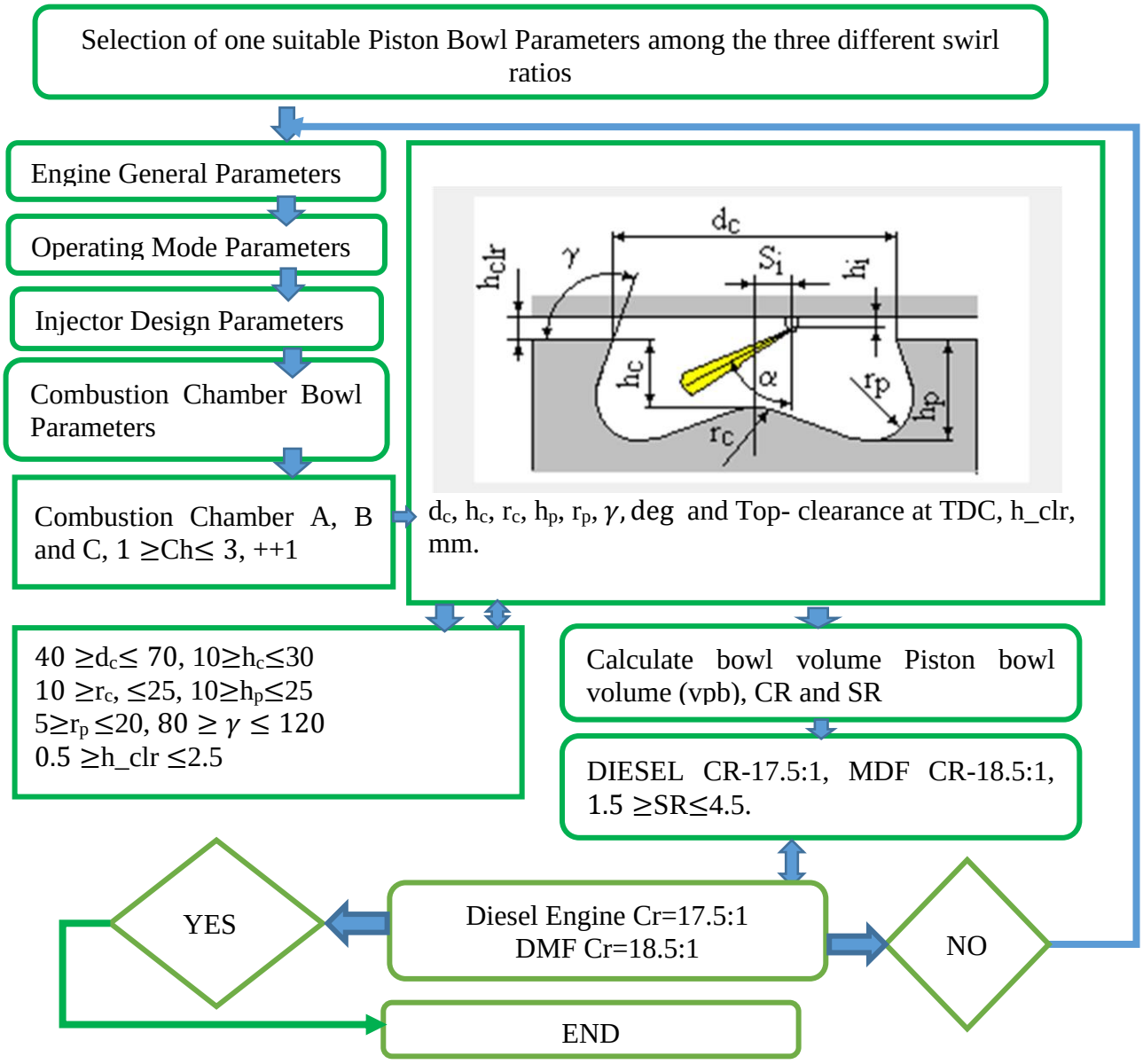


Figure 2.3 selection methodology of Combustion chamber bowls

Combustion bowl parameters selection and prediction is significant to approach and obtained by simulation as shown in Figure 2.3. Combustion chamber parameters like **$d_c$, $h_c$, $r_c$, $h_p$, $r_p$ $\gamma$, deg** and Top- clearance at **TDC, h_clr**, mm shown in Table 1. Swirl ratio (SR) depends on the movement of fresh charge (e.g., air) around the cylinder axis in the cylinder of IC engine. CI engine piston bowl parameters er highly influence SR, and it is inessential mixture preparation and initiating combustion MDF air mixture in CI mode engine[5]. Dc varies from 55.2 to 65.2 mm, and geometry parameters details are shown in Table 1. Bowl surface area is.

.

 https://doi.org/10.37896/pd91.3/91329

ISSN: 0369-8963
PERIODICO di MINERALOGIA Volume 91, No. 3, 2022

TABLE: 1 The Combustion Chambers Parameters (DMF Fuel Cr-18.54:1)

| **Description** | **Chamber-A** | **Chamber-B** | **Chamber-C** | |
|---|---|---|---|---|
| 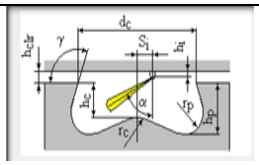 | 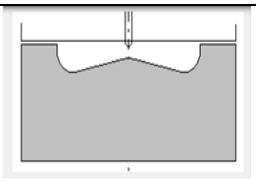 | 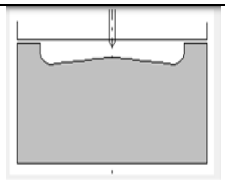 | 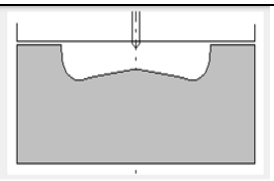 | |
| Description | | CH-A | CH-B | CH-C |
| dc - External Diameter (mm) | | 58.2 | 65.2 | 55.2 |
| Hc- Piston bowl depth, (mm) | | 4 | 4 | 7 |
| Rc -Radius of the sphere the in centre of piston bowl, (mm) | | 4 | 4 | 7 |
| Hp - Depth of combustion chamber in the periphery (mm) | | 8.1 | 6.1 | 10.1 |
| Rp - Radius of the hollow chamber in the periphery of bowl, (mm) | | 6.31 | 4.31 | 6.31 |
| Gamma (***γ***) | | 99 | 101 | 84 |
| h_clr - Top-clearance at TDC, (mm) | | 1.001 | 1.00 | 1.00 |
| SR | | 2.9 | 2.3 | 3.1 |

The diesel RK tool simulated three different combustion bowl chambers, A, B, and C, under all operating conditions. Swirl ratio significantly impacts in-cylinder combustion, soot formation, and heat release rate. Fuel evaporation and combustion are affected by injection pressure, in-cylinder pressure and temperature, combustion chamber air turbulence and swirl ratio [7]. The air flow near Bottom Dead Center (BDC) during the intake process increases during the compression stroke [8].

This phenomenon significantly impacts combustion and soot formation [9]. The swirl ratio and squishes in the combustion chamber affect flame propagation by breaking up fuel droplets and spreading the flame front [10]. The diesel RK parameter optimisation methodology was used to determine the best parameters, including compression ratio, swirl ratio, injection timing (IT), swirl ratio, and injection pressure with and without EGR [11]. Some important parameters such as compression ratio, injection timing, injector nozzle diameter, number and direction, combustion bowl chamber shape, valve timing, and turbocharging parameters are predicted [12]. [13][14].

Performance parameters such as SFC, ID, EGR, swirl ratio, injection timing, and the extremum of a goal function are optimised for improved combustion. As a result, the numerical experiment is affected by the influence of many variables involved in better combustion. [15]. Previous research suggested that non-linear programming is excellent for predicting multi-parametric optimisation and for selecting appropriate parameters [16]. [17] [3]. A mathematical model connects independent variables (optimisation parameters) with goal functions and some constraints for parameter prediction. [18]. Efficiency, ignition delay, IMEP, and SFC are some of the parameters that can be included in the goal function of the Diesel RK simulation software [19]. [20]

 https://doi.org/10.37896/pd91.3/91329

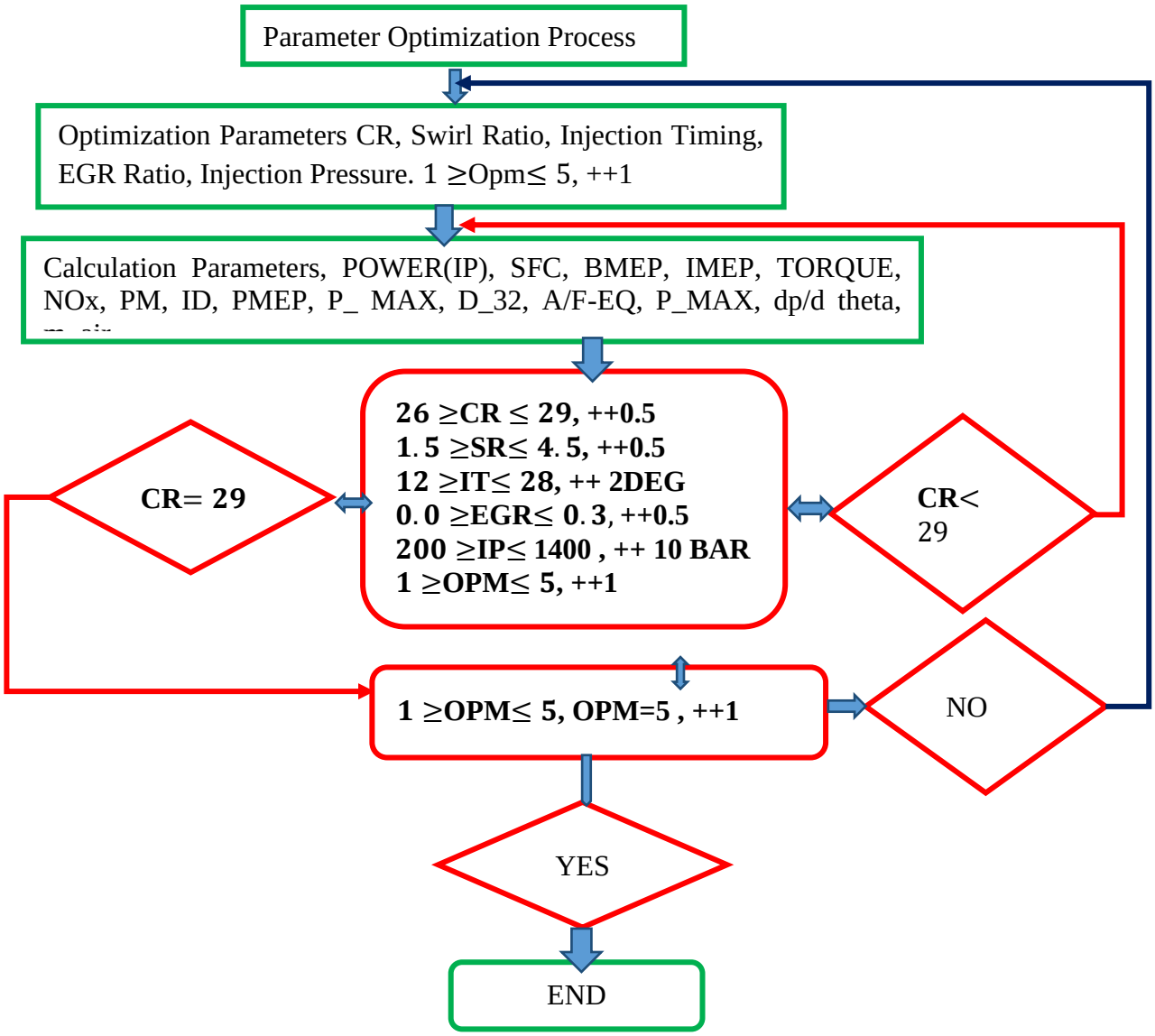


Figure 2.4 Diesel RK Optimization Process

Optimal parameters Specifically, $X_k$ is a variable that represents a set of design data for a CI engine. These design data include things like the compression ratio (CR) and the injection timing, among other things. An extremum value of the objective function can be anticipated by simulation based on the selection of parameters and the importance of these data.

$$Z_j = Z_j(X_k) \quad \text{--------} \quad (1)$$

Critical According to the authors, several essential design factors are being sought to find the best possible IC engine. Monitoring of the engine's thermal and mechanical parameters is required, along with some upper and lower bounds. [21].

$$Y_i = Y_i(X_k) \quad \text{----------} \quad (2)$$

When calculating a goals function like the one used in this study (SFC), there is no mathematical relationship between the SFC's limitations and the vector of explanatory variables. Simulating and searching for an optimal value of a function $Z_j$ ($X_k$) in the presence of constraints reduces the complexity of optimisation problems:

 https://doi.org/10.37896/pd91.3/91329

$$Y_{imin} < Y_i(X_k) < Y_{imax} \quad (3)$$

Conditional and non-conditional optimisation issues can be reduced using methods that are better equipped for optimisation because of the limits that make solving them more difficult. It is possible to consider limits in predicting suitable parameters using the penal function method. In this system, if a target is exceeded, a penalty is imposed, and the objective is reduced to its possible value. The penalty will rise in proportion to the save of the infringement. The notation (F) is typically a combination of C item.,, $F = C_{zj}.Z_j + \sum_{i=1}^{n} C_{yi}.\Delta Y_I^2) + \sum_{K-1}^{m} C_{xk}.\Delta X_k^2$ ) --- (4)

$C_{zj}$Is a line factor (influence coefficient) of optimised ICE parameter $Z_j$ included in goal function? $Z_j = \frac{Z_j}{Z_{j-mean}}$ Is a relative ICE parameter $Z_j$ related to its mean average value (for example: SFC, power, NO emission, etc.); $C_{yi}$ is a penal factor for leaving permitted area of $\Delta Y_i = \begin{cases} \frac{Y_i - Y_{imin}}{Y_{imean}}, IFY_i < Y_{imin} \\ 0, \quad IF\ Y_{imin} \le Y_i \le Y_{imax}, \\ \frac{Y_i - Y_{imax}}{Y_{imean}}, Y_i > Y_{imax} \end{cases}$, is a related value of violation of restriction $Y_i$; $C_k$ is a penal factor for leaving permitted area of $X_k$ $\Delta X_k = \begin{cases} \frac{X_k - X_{kmin}}{X_{kmean}}, IFX_k < X_{kmin} \\ 0, \quad IF\ X_{kmin} \le X_k \le X_{kmax}, \\ \frac{X_k - X_{kmax}}{Y_{kmean}}, X_k > X_{kmax} \end{cases}$, is a related value of $X_k$ lapped over allowable borders;

The programme selected the $X_{k\ to\ mean}$ values of explanatory variables and constraints, $Y_i$ and punitive factors of $X_k$ by the programme and applied the specification of penal elements for restrictions. C. The user in the pre-processor must set the most and least permissible limits in a restriction Yi min, Yi max, Xi max, and Zj target function. [23]. To identify optimal parameters for a position with numerous variables, well-known nonlinear programming algorithms from a library are employed. [24]. NLP theory doesn't tell you which strategies are better to use in the selection process. [25].

## DIESEL-RK LIBRARY ALGORITHMS

Methods like the One-coordinates descent method, the Deformable polyhedron method, the Rosenbrok method, and the Powell method are already included within the simulation tool. These are just a few examples. This is the shortest descent method used for partial derivatives of the objective function. Heavy ball technique, Fletcher Reeves method, Polak-Ribier method, Projective Newton-Rafson method, Davidon-Fletcher-Powell method, Broaden method, Pearson 2 method, Pearson 3 method, Random search method, and Monte Carlo method are all methods incorporated into the simulation engine itself. Optimisation of combustion,

 https://doi.org/10.37896/pd91.3/91329

performance, and emission characteristics can be achieved using any of the provided algorithms.

TABLE: 2. The Optimum Parameters of Experiments And Simulation.

| FUEL | CR | SR | IT (Deg, BTDC) | EGR RATIO | INJECTION PRESSURE (BAR) |
|---|---|---|---|---|---|
| DIESEL | 17.5:1 | 3.2 | 23 | 0.15 | 800 |
| DMF | 18.54:1 | 2.9 | 20 | 0.15 | 800 |

### *B Experimental setup*

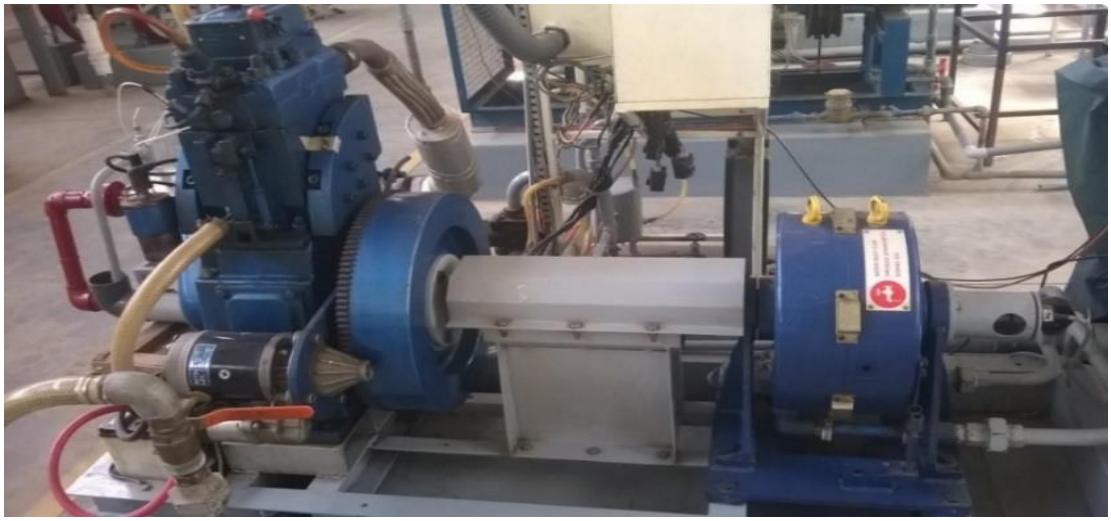

Figure 2.5 Experimental setup

**TABLE: 3 Technical Specification of Eddy Current Dynamometer**

| | |
|---|---|
| Dynamometer Model and Make | AG-10, SAJ Test Plant Pvt. Ltd |
| End flange both sides | Carbon shaft model 1260 type A |
| Cooling Water inlet pressure, kg/cm$^2$, and Air gap mm | 1.6 to 2, and 0.77/0.63 |
| Torque Nm | 11.5 |
| Dynamometer Speed range | 500 to 5000 RPM |

To conduct the trials, we used an Eddy Current Dynamometer (ECD) to measure the engine's output at 1500 RPM. Several experiments were carried out to verify the results of the simulation studies in this research. Exhaust Gas Recirculation (EGR) and other measurement systems were linked with the core system, the Variable of Compression Ratio, ignition delay, SFC, and BTE of the Engine in the experimental setup depicted in Figure 2.5.

NI-DAQ connects various measurement instruments, including an eddy current dynamometer, crank angle encoder, in-cylinder pressure sensors, and fuel and airflow sensors. This specification includes information on the NI-DAQ data acquisition systems, which collect

 https://doi.org/10.37896/pd91.3/91329

engine performance and emission data. With and without EGR, chamber A's experimental validation and in-cylinder pressure change were discussed [27].

## Results And Discussion

### *A.* SFC Vs Injection Pressure

Experiments and simulation results are used to detect the variance in SFC with increasing injection pressure better to understand the effect of increased injection pressure on SFC. Figures 3.1 and 3.2 illustrate a range of injection pressures from 600 to 1400 bar with EGR varying from 0% to 15%. In this part, some graphs are given, and the results are summarized in Table 3.2

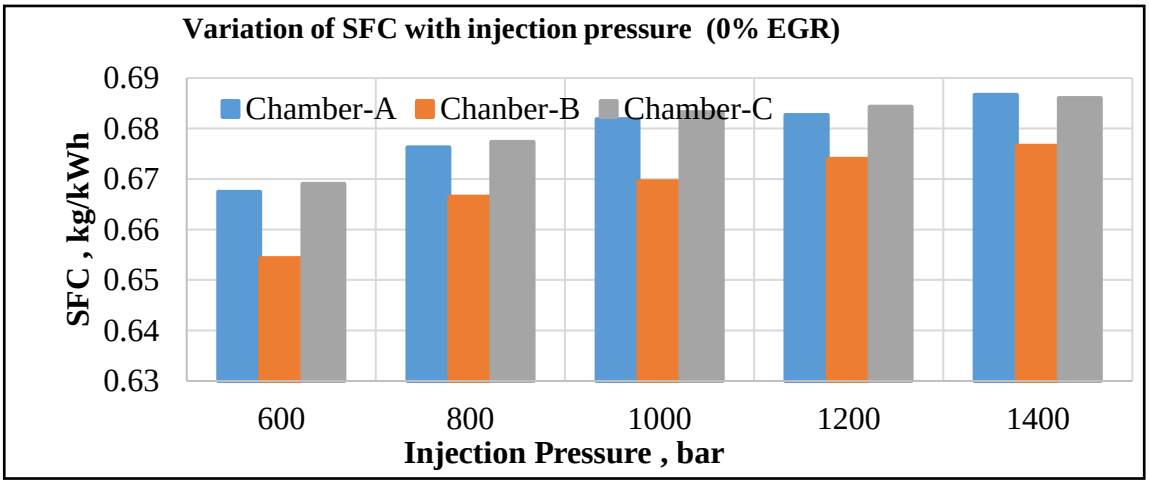


Figure 3.1Variation of SFC with Variation of injection pressure - 0% EGR

Based on the simulation results, the following parameters are obtained, SFC of Chamber A with 0% EGR is raised from 0.669 to 0.686 kg/kWh. SFC of 15% EGR mode increased from 0.706 to 0738 kg/kWh when injection pressure increased from 600 to 1400 bar. The SFC of Chamber C with 15% EGR mode is 8.23 % higher than 0% EGR. SFC of Chamber-B is 2.24% is lower compared to Chambers C, and 2 % is lower compared to Chamber A at 600 bar pressure.

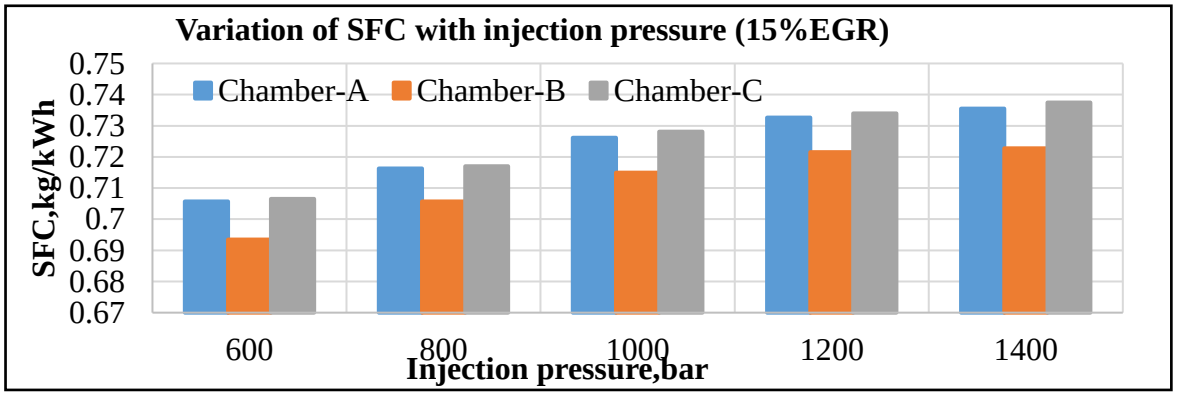


Figure 3.2 Variation of SFC with various injection pressure - 15% EGR


https://doi.org/10.37896/pd91.3/91329

When injection pressure is increased from 800 to 1400-bar pressure, SFC in Chamber B is 1.42 per cent lower than in Chambers A and C. When the injection pressure is raised in either the 0% EGR or 15% EGR modes, the SFC of all three chambers increases. Figures 3.1 and 3.2 demonstrate that Chamber B and C's similar trends. Chamber B's SFC, on SFC, followed other hand, is a whopping 1.6 to 2.2 percentage points lower than that of Chambers A and C. Due to more excellent combustion and heat release, Chamber -A generates 0.3kW more power than the other two chambers. The results of this investigation have led to certain conclusions. Chamber A's 15% EGR mode has a 7.1% better efficiency than Chamber A's 0% EGR mode. In the 15 per cent EGR mode, SFC increases from 0.706 to 0.738 kg/kWh, whereas in Chamber B, the SFC goes up from 0.654 to 0.677 kg/kWh. 3) Comparing Chamber B with 15% EGR mode to 0% EGR mode, an 8.2% increase is seen.

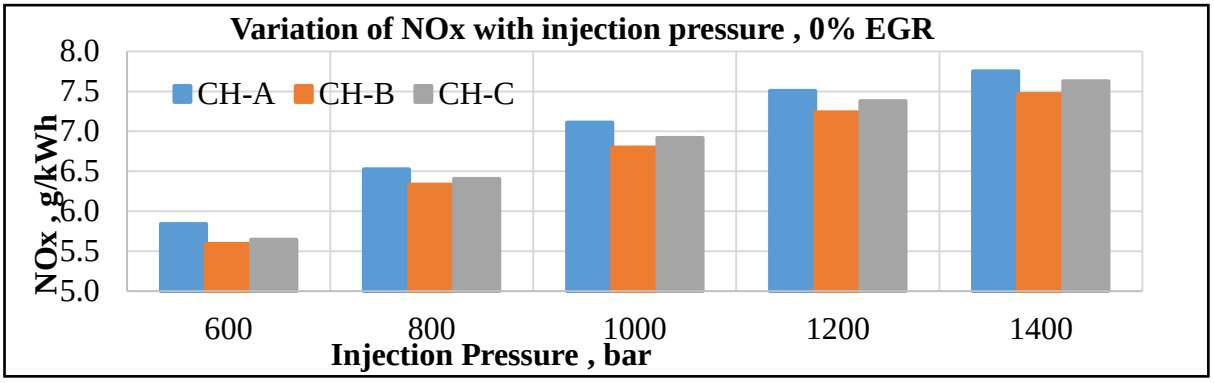


Figure 3.3Variation of NOx with various injection pressure - 0%EGR

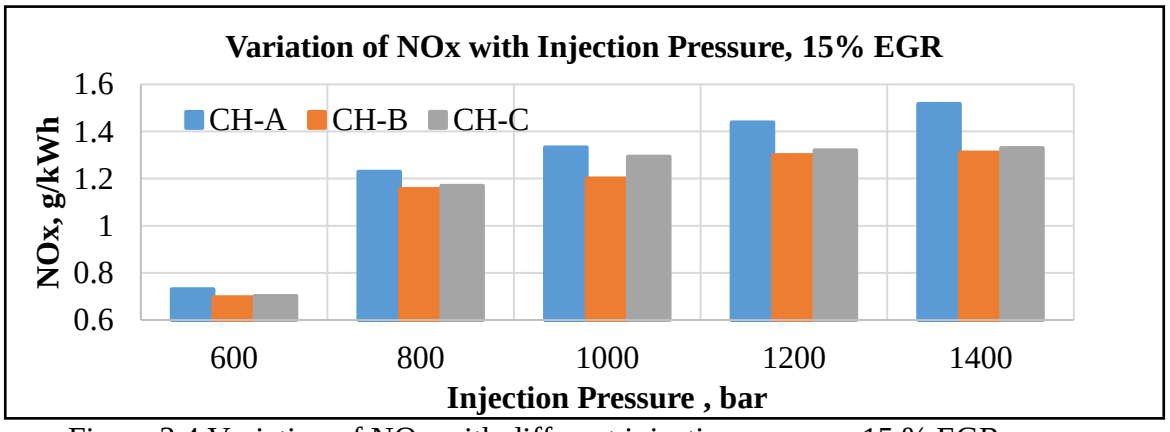


Figure 3.4 Variation of NOx with different injection pressure-15 % EGR

Injection pressure increases from 600 to 1400 bar, increasing the NOx in Chamber A from 5.838 to 7.751 g/kWh while operating in 0% EGR mode. This increases to 1.52 g/kWh when running in 15% EGR mode, as illustrated in Figures 3.3 and 3.4. Compared to a 0 percent EGR mode, the NOx emissions from Chamber A are 80.2% lower when operating in 15 percent EGR mode. Chamber B's NOx emissions increased from 5.644 to 7.5 g/kWh in the 0 percent EGR mode based on the combustion simulation findings. Chamber C's NOx emissions ranged from 5.62 to 7.63 g/kWh with no EGR, whereas Chamber B's NOx emissions ranged from 0.71


https://doi.org/10.37896/pd91.3/91329

to 1.33 g/kWh with 15% EGR, and Chamber C's NOx emissions ranged from 0.712 to 1.34 g/kWh with 15% EGR.

Figure 3.5Variation of ID with various injection pressure – 0 %EGR

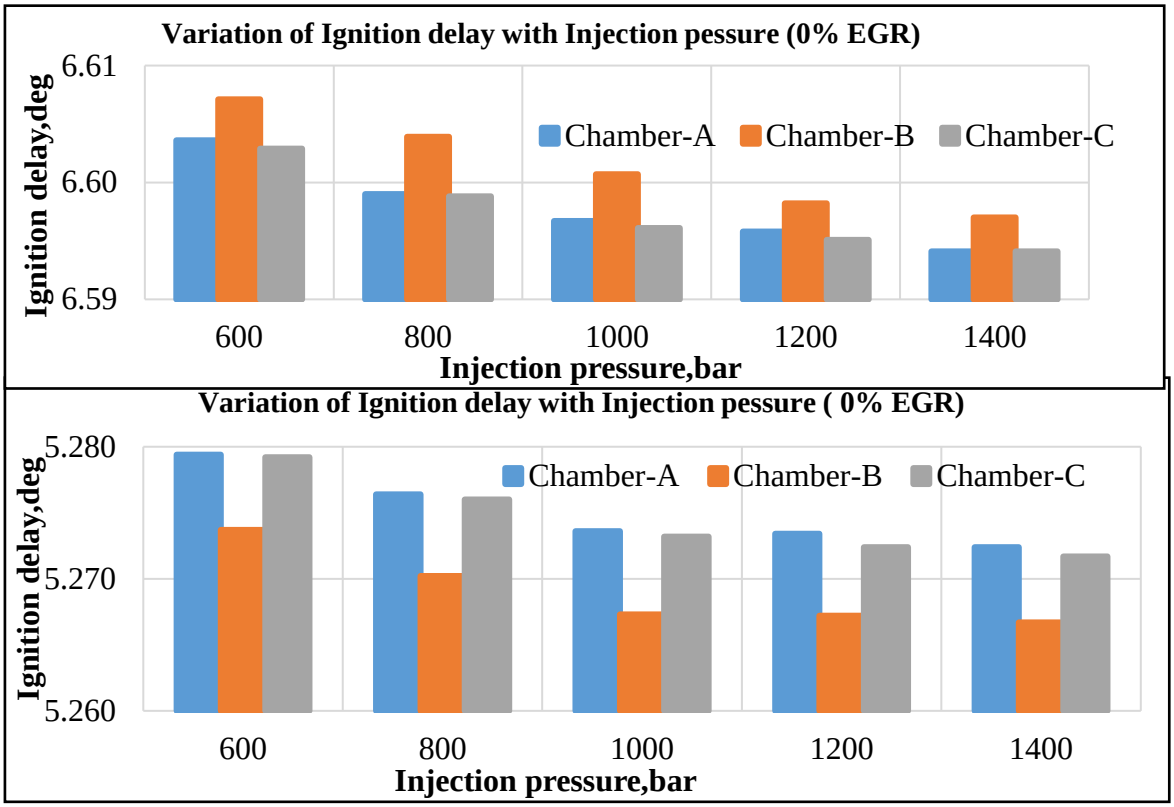


Figure 3.6Variation of ID with different injection pressure-15 % EGR

NOx of Chamber B with 15% EGR mode is 81.72 % decreased, and Chamber C is 82.2% decreased compared to 0% EGR mode, as shown in Figure 73. NOx of Chamber B is lower compared to the other two Chambers A and C. Variation of CFM, SOI and SOC of MDF and rate of pressure rise are valuable information of combustion of HCI engine. In-cylinder peak pressure of HCI engine combustion Chamber A is nearly 32 bar higher than the base engine due to the high compression ratio. Hence in-cylinder pressure and temperature increased. In-cylinder pressure variation with CA gives valuable information about the peak pressure of the combustion and pressure force acting on the piston with CA[28]. SOI and SOC are identified, injection started from BTDC 23 deg, and combustion started from BTDC 17 deg[29]. The Peak Pressure of the explosion is attained near ATDC, and the driving force acting on the piston due to the rate of pressure rise is high, and the heat release rate increases during this period[30].

The Diesel RK heat release model to predict the heat release rate and plotted with CA, shown in Figure 3.7. The variation of HRR with CA is shown in Figure 3.7. Simulation results are used to find the interpretation of HRR, plotted concerning CA, and compared with different CFM, which varied from 0.01776 to 0.0338g/cycle.3.3. Summary of Three Different Combustion Chambers A, B and C for MDF Fueled HCI Engine. Based on the

 https://doi.org/10.37896/pd91.3/91329

simulation results, the outline of performance and analysis of Chambers A, B and C for the HCI engine are arrived at, detailed result analysis, and presented.

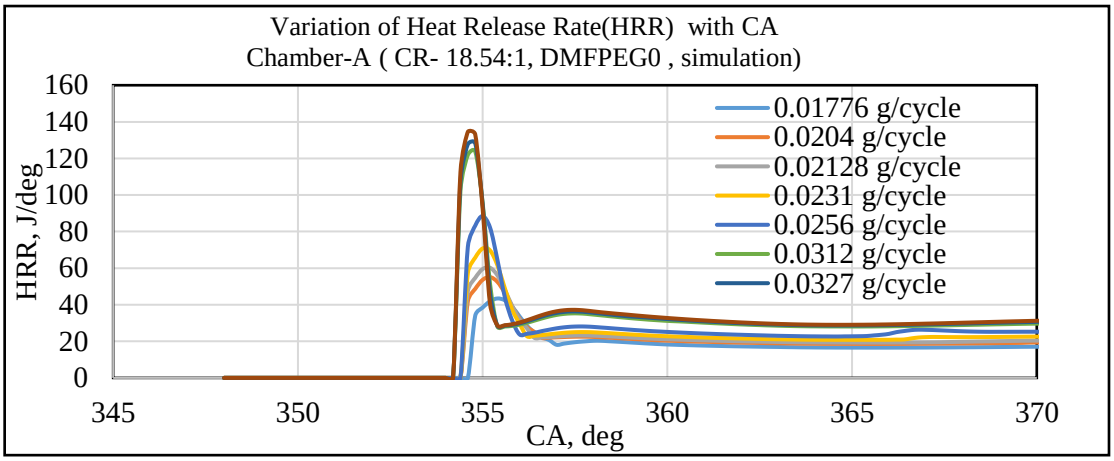


Figure 3. 7 Variation of Heat Release Rate (HRR) with CA Chamber-A (CR- 18.54:1, DMF)

SFC, NOx and Ignition delay of fuel is the critical parameters and find the knocking characteristics of HCI engines. Ignition delay depends upon many factors such as in-cylinder pressure, compression ratio, the inlet pressure, injection parameters, EGR and the properties of the fuel[31]. Higher the CN, the shorter the ignition delay, and vice versa. In-cylinder peak pressure of Chamber A, B and C for load 3.9 kW is shown in Table 1. Heat release rate with CA, Comparison of SFC, NOx, PM and ID with different CFM at 1400 bar injection pressure for Chambers A, B and C are shown in Table 1 and

TABLE: 4 Heat Release Rate with Ca Degree

| Heat release rate (HRR) | CH-A, Max. Load, (3.9 kW) | CH-B | CH-C |
|---|---|---|---|
| Premixed heat release rate (kJ/deg) | 123.4 | 127.7 | 197.4 |
| The premixed zone- heat release rate Peak value (%) | 2.36% > B<br>37.56 < C | 2.36 < A<br>55.1% < C | 37.53>A<br>55.1 > C |

Based on the simulation results, the Heat Release rate (HRR) of Chamber A, B and C with different CFM and plotted concerning Crank Angle (CA) and discussed in section 3.0. It was found that from Table 4, the premixed heat release rate was compared at maximum load. HRR of Chamber A is 2.36%, 37.53 lower than Chamber B and C for a whole load of 3.9kW. MDF evaporation rate is directly involved in an in-cylinder peak temperature and controlled using EGR. SFC, NOx, PM and ID of Chambers A, B and C with different CFM are plotted with extra injection pressure and discussed in section 3. SFC, NOx, PM and ID of Chambers A, B and C results with additional CFM and vary from 0.01776 to 0.0338 g/cycle for 1400 bar injection pressure shown in Table 5.

 https://doi.org/10.37896/pd91.3/91329

TABLE 5 SFC, NOX, PM and Id Comparison 0f Chambers A, B And C For 1400 Bar Injection Pressure

| COMBUSTION CHAMBER | SFC, NOx, PM and ID Comparison of Chambers A, B and C for 1400 bar injection pressure | | | |
|---|---|---|---|---|
| **CFM-0.01776 g/cycle** | | | | |
| CHAMBER | SFC g/kWh | NOx g/kWh | PM g/kWh | ID g/kWh |
| CH-A | **1.6%>B** | **4.1%>B** | **0.001** | **0.115>B** |
| CH-B | 1.6%<A and C | 4.1% < C and A | < 0.001 | 0.1%<A and B |
| CH-C | 2.2%>B | 4.2>B | 0.0001 | 0.11%>C |
| CFM **0.02128 g/cycle** | | | | |
| | SFC | NOx | PM | ID |
| CH-A | **5.9>B** | **4.2%>B** | **0.001** | **0.116%<B and C** |
| CH-B | 5.9%,<A and C | 4.2% < A and C | <0.001 | 0.11%>A |
| CH-C | 5.9%>B | 4.2% > B | | 0.11%>B |
| **CFM 0.0256 g/cycle** | | | | |
| | SFC | NOx | PM | ID |
| **CH-A** | **1.9%>B** | **5.8%> B** | **0.001** | **0.12%<B and C** |
| CH-B | 1.9%<A and C | 5.8% < A and C | <0.001 | 0.12%>A |
| CH-C | 1.9%>B | 5.8%> B | <0.001 | 0.12%>A |
| **CFM 0.0327 g/cycle** | | | | |
| | SFC | NOx | PM | ID |
| CH-A | **1.9>B** | **5.6%> B** | **0.001** | **0.11%<B and C** |
| CH-B | 1.9%,<A and C | 5.6%<A and C | <0.001 | 0.11%>A |
| CH-C | 1.9%>B | 5.6% >B | <0.001 | 0.11%>B |
| CFM0.0338 g/cycle | | | | |
| | SFC | NOx | PM | ID |
| CH-A | 1%>B | 2%>B | 18.2 < B | 0.15>B |
| CH-B | 1%<A and C | 1.98% <A | 18.2%>A | 0.15<A |
| CH-C | 1%>B | 2%>B nearly equal to A | 20%>C (Low soot) | 0.15>B |

In-depth analysis of performance aspects results in comparison graphs. When injection pressure climbs from 600 to 1400 bar, SFC increases by 5.4 percent in Chamber A and 7.2 percent in Chamber B when operating in 15 percent EGR mode. Chambers A, B, and C all have the same SFC pattern. Chamber B's SFC is about 1.6 to 2.2 percent lower than the other chambers A and C [28]. The NOx emissions in Chamber A with 15% EGR mode are 87.1

 https://doi.org/10.37896/pd91.3/91329

percent, 87.2 per cent, 86.2 per cent, 85.6 per cent, and 85.2 per cent lower than when the chamber is not using EGR mode when the injection pressure is raised from 600 to 1400 bar. Based on these findings, the following was concluded: When using EGR, the SFC of Chamber A is a little bit greater than when without EGR.; Chamber A, With 15% EGR mode, has a lower NOx emission rate than other chambers. Section 3.0 shows that in 15 per cent EGR mode, Chamber A's ID is lower than the IDs of the other Chambers. One of the most critical parameters in HCI mode combustion is the ignition delay (ID). That means Chamber A has a lower ID than the other chambers. The reduced ID[32] is one of the advantages over other parameters. After a thorough investigation, Combustion Chamber A was chosen as the best option for an MDF-powered HCI engine for a given piston. Tests were performed with and with EGR without Experiment data to verify the combustion chamber A [33] simulation.

## Experimental Validation of Base Fuel Engine Combustion Chamber-A.

### *A. Experimental Validation of In-Cylinder Pressure with C A of Chamber-A*

In-cylinder pressure with CA of the diesel engine of Chamber A with 0% EGR simulation results.

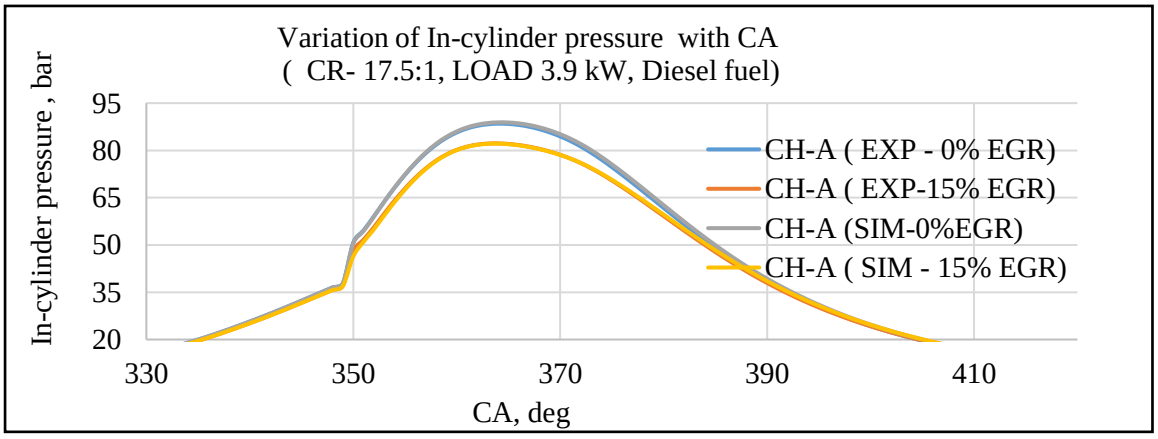


Figure 4.1 Variation of In-cylinder pressure with CA (degree) (CR- 17.5:1, LOAD 3.9 kW)

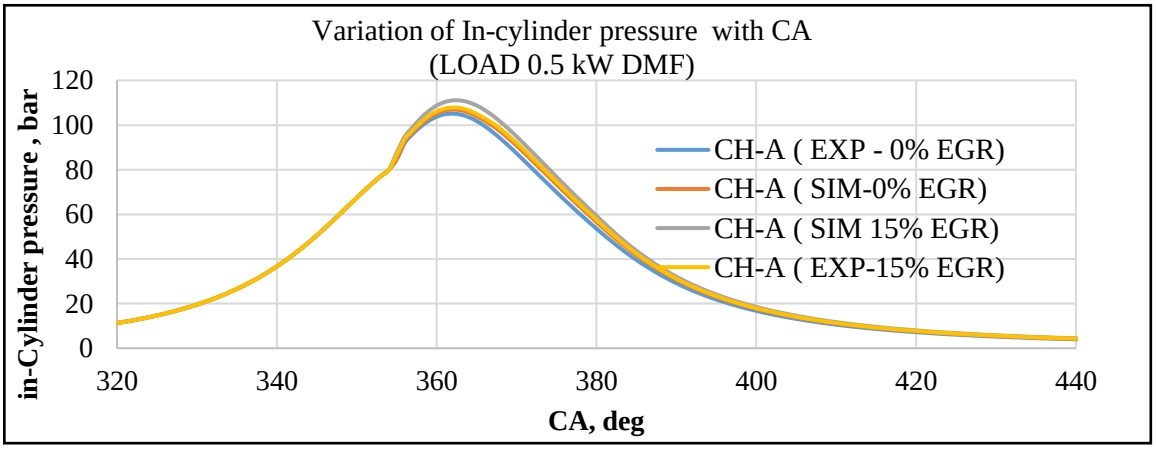


 https://doi.org/10.37896/pd91.3/91329

Figure 4.2 Variation of In-cylinder pressure with CA (CR- 18.54:1, LOAD 0.5 kW)

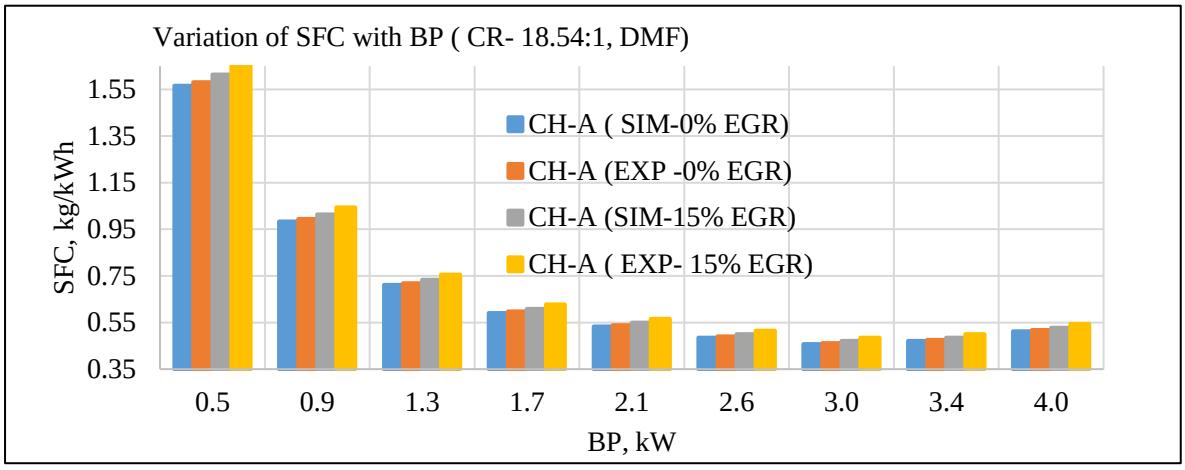


Figure 4.3 Variation of SFC with BP (CR- 18.54:1, DMF

The peak pressures measured inside the cylinders match those measured in experiments. Chamber A's simulation results with a 15% EGR simulation accord well with the results of the trials. Compared to experimental in-cylinder pressure, CA in-cylinder pressure rises from 0.8 to 1.2 per cent. Figure 4.1 depicts the results of experiments carried out in a particular combustion chamber A. Chamber A's CA with 0 per cent EGR simulation findings were compared to those of trials at 3.9kW load for in-cylinder pressure. [34].
The in-cylinder peak pressures of 0% EGR simulation are in good agreement compared with 0% EGR experimental at 3.9kW load. Chamber A with 15% EGR simulation results are compared with CH-A with 15% EGR experimental results, and there is a good agreement.

***B. Validation of SFC with BP for Standard Piston (STDP) and Chamber-A***

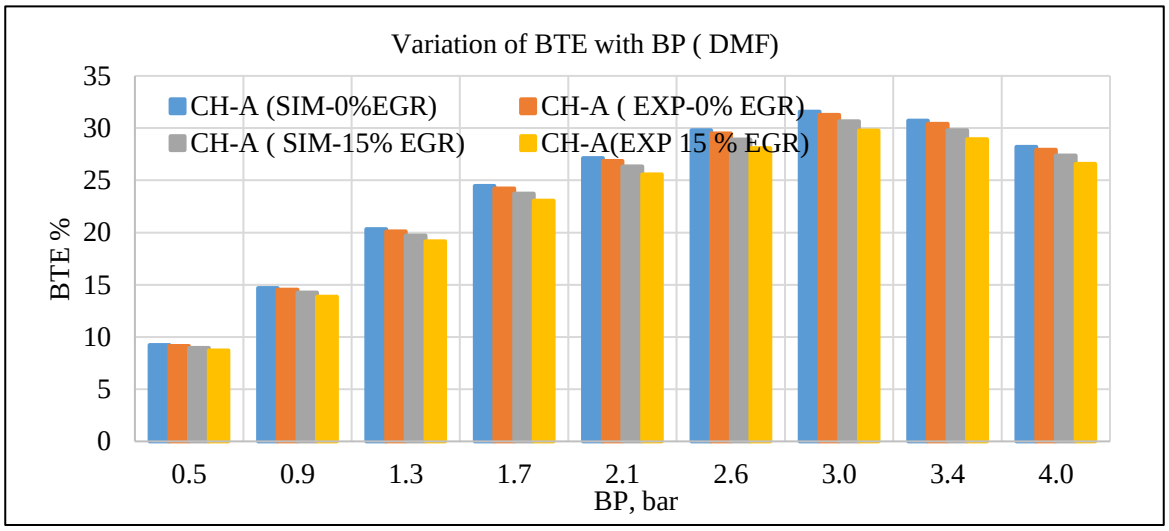


Figure 4.4 Variation of BTE with BP (DMF fuel, RPM 1500, CR, 18.54:1)

 https://doi.org/10.37896/pd91.3/91329

Comparing simulation findings with CH-A with 15% EGR experimental data, the results are shown in Figure 4.1, and they are in good agreement with each other. Figure 4.1 shows an increase in practical in-cylinder pressure with a CA diagram of 0.7 and 1.1 per cent in in-cylinder pressure with CA. From 0.99 kg/kWh to 0.33 kg/kWh, the SFC of the base engine has been reduced significantly. There is a decrease in the SFC of the MDF engine from 1.54 to 0.50 g/kWh. Comparing Chamber A's SFC, BTE and NOx with and without EGR simulation results, the results of trials were plotted. Compared to experimental results, the SFC of simulations is in good accord.

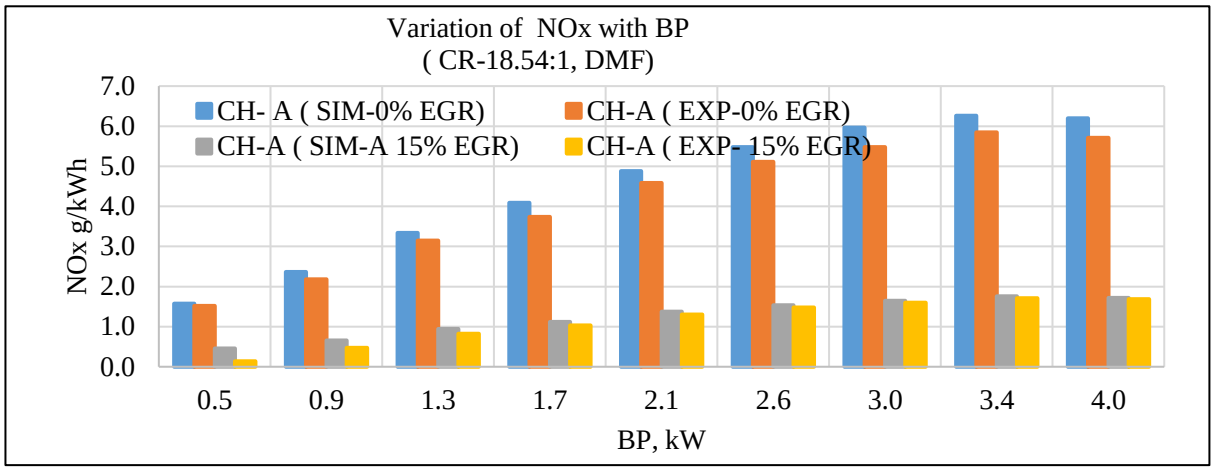


Figure 4.5 Variation of NOx with BP of Chamber A

As shown in Figure 4.5, Chamber A with 15 per cent EGR simulation results is compared to Chamber A with 15 per cent EGR experimental findings. The results are similar, as evidenced by the SFC and BTE data. Figure 4.4 shows that they are in complete agreement. Figure 4.5 compares the NOx emissions from the CH-A and Chamber A tests using a 15% EGR simulation and experimental data from the last chamber. STDP experimental NOx measurements with 15% EGR are about 0.5 to 1.5 per cent lower than STDP simulations with 15% EGR. Compared to STDP with 0 per cent EGR simulation, NOx of STDP with 0 per cent EGR experimental is roughly 0.5 to 2.5 per cent lower.

## Conclusion

The following conclusion is based on the results of both simulations and experiments. Experimental shows data on SFC, NOx, PM, and ID for three distinct CFM combustion chambers with injection pressures ranging from 600 to 1400 bar. Table 4 displays the SFC, NOx, PM, and ID for Chambers A, B, and C at 1400 psi injection pressure.

2. Chamber A's SFC is 3.36 per cent greater than Chamber B and C because of the higher evaporation rate and heat release rate at 1400 pressure. At 1400-bar injection pressure, chamber A's premixed combustion zone heat release rate is more significant than chambers B and C, as indicated in the sample data comparison tables 3.1 and 3.2.


https://doi.org/10.37896/pd91.3/91329

The following findings can be drawn from an in-depth investigation: A 15 per cent EGR mode results in a slightly higher SFC for Chamber A at all CFM. Compared to other chambers with varying injection pressures, the amount of NOx in Chamber A with a 15% EGR mode is lower. As illustrated in this paper, other Chambers at different CFMs have a lower PM and a lower ID than Chamber A at different CFMs. Chamber A's standard ID is one of the additional benefits of other selection characteristics.

The DMF fuel engine's combustion chamber A was chosen after a thorough investigation. Another experiment was carried out with and without EGR in Combustion Chamber A. Combustion Chamber A models for the DMF direct injection high compression ignition engine is validated using the experimental results.

## Nomenclature

| | | | | | |
|---|---|---|---|---|---|
| $U_p$ | | Average Piston Speed | IP | - | Indicated Power |
| BDC | | Bottom Dead Center | ITE | - | Indicated Thermal Efficiency |
| BMP | - | Brake Mean Effective Pressure | IDI | - | Indirect Injection |
| BP | - | Brake Power | ICE | - | Internal Combustion Engine |
| BSFC | - | Brake Specificuel Consumption | ISO | - | International Standard Organization |
| BTE | - | Brake Thermal Efficiency | MTBE | - | Methyl Tetra Butyl Ether |
| $CO_2$ | - | Carbon Dioxide | NWR | - | Near Wall Flow |
| CO | - | Carbon Monoxide | NOx | - | Nitrous Oxide |
| CN | - | Cetane Number | NDIR | - | Non-Dispersive Infrared Analyzer |
| CR | - | Compression Ratio | PM | - | Particulate Matter |
| CFR | - | Cooperative Fuel Research | PEG | - | Poly Ethylene Glycol |
| CA | - | Crank Angle | SFC | - | Specific Fuel Consumption |
| CFM | - | Cycle Fuel Mass | SOC | - | Start of Combustion |
| DI | - | Direct Injection | SOI | - | Start of Injection |
| | | | SR | - | Swirl Ratio |
| EGR | - | Exhaust Gas Recirculation | $U_t$ | - | Swirl Tangential Speed |
| FP | - | Friction Power | TDC | - | Top Dead Center |
| GHG | - | Greenhouse Gas | TFC | - | Total Fuel Consumption |
| HSU | - | Hartridge Smoke Unit | UHC | - | Unburned Hydro Carbon |
| HC | - | Hydro Carbon | HRR | - | Heat Release rate |
| IMEP | - | Indicated Mean Effective Power | | | |

## ACKNOWLEDGEMENT

I wish to record my deep sense of gratitude and profound thanks to my research supervisor, **Dr A.S. Krishnan., Dr G SureshKannan.,** Associate Professor and **Dr K. Marimuthu,** Head of the Department of Mechanical Engineering, Principal, Coimbatore Institute of Technology, Coimbatore-641014, for his keen interest in timely motivation, inspiring guidance and constant encouragement with my work during all stages, to complete the research successfully.

 https://doi.org/10.37896/pd91.3/91329

## Reference

[1] J. L. Da Silva and M. Aznar, "Thermophysical properties of 2,5-dimethylfuran and liquid-liquid equilibria of ternary systems water + 2,5-dimethylfuran + alcohols (1-butanol or 2-butanol or 1-hexanol)," *Fuel*, vol. 136, pp. 316–325, 2014, DOI: 10.1016/j.fuel.2014.07.039.

[2] Z. Gao, E. Hu, Z. Xu, G. Yin, and Z. Huang, "Effect of 2,5-dimethylfuran addition on ignition delay times of n-heptane at high temperatures," *Front. Energy*, vol. 13, no. 3, pp. 464–473, 2019, DOI: 10.1007/s11708-019-0609-z.

[3] M. Velliangiri, G. Sureshkannan, M. Karthikeyan, and K. Karthik, "Prediction of Suitable Ignition Timing and Compression Ratio of Dmf Direct Injection Turbocharged Multi-Cylinder Si Engine with EGR," vol. 5, no. 7, pp. 6–16, 2019.

[4] P. Zhang, X. Su, H. Chen, L. Geng, and X. Zhao, "Assessing fuel properties effects of 2,5-dimethylfuran on microscopic and macroscopic characteristics of oxygenated fuel/diesel blends spray," *Sci. Rep.*, vol. 10, no. 1, pp. 1–12, 2020, DOI: 10.1038/s41598-020-58119-y.

[5] " The Effect of Swirl Ratio and Fuel Injection Parameters on CO Emission and Fuel Conversion: S. Kook, C. Bae, P. C. Miles, D. Choi, M. Bergin, and R. D. Reitz, "The Effect of Swirl Ratio and Efficiency for High-Dilution, Low-Temperature Combustion in an Automotive Diesel Engine," Apr. 2006, DOI: 10.4271/2006-01-0197.

[6] E. Porpatham, A. Ramesh, and B. Nagalingam, "Effect of swirl on the performance and combustion of a biogas fuelled spark ignition engine," *Energy Convers. Manag.*, vol. 76, pp. 463–471, 2013, DOI: 10.1016/j.enconman.2013.07.071.

[7] M. F. Al-Dawody and S. K. Bhatti, "Effect of variable compression ratio on the combustion, performance and emission parameters of a diesel engine fuelled with diesel and soybean biodiesel blending," *World Appl. Sci. J.*, vol. 30, no. 12, pp. 1852–1858, 2014, doi: 10.5829/idosi.wasj.2014.30.12.338.

[8] G. Chen, L. Di, Q. Zhang, Z. Zhang, and W. Zhang, "Effects of 2, 5-dimethylfuran fuel properties are coupling with EGR ( exhaust gas recirculation ) on combustion and emission characteristics in common-rail diesel engines," *Energy*, vol. 93, no. x, pp. 284–293, 2015, DOI: 10.1016/j.energy.2015.09.066.

[9] M. P. Sudeshkumar and G. Devaradjane, "Development of a Simulation Model for Compression … DEVELOPMENT OF A SIMULATION MODEL FOR COMPRESSION IGNITION ENGINE RUNNING WITH IGNITION IMPROVED BLEND," vol. 15, no. 4, pp. 1131–1144, 2011, DOI: 10.2298/TSCI100717043S.

[10] K. Hareesh, R. T. N, and B. K. Reddy, "Computer Simulation of Compression Ignition Engine through MATLAB," *Int. J. Res. Appl. Sci. Eng. Technol.*, vol. 995, no. 2, pp. 2321–9653, 2014, Accessed: Dec. 23, 2016. [Online]. Available: www.

[11] C. D. Rakopoulos, G. M. Kosmadakis, A. M. Dimaratos, and E. G. Pariotis, "Investigating the effect of crevice flow on internal combustion engines using a new simple crevice model implemented in a CFD code," *Appl. Energy*, vol. 88, no. 1, pp. 111–126, 2011, DOI: 10.1016/j.apenergy.2010.07.012.

[12] V. Murugasen and K. AnnurSrinivasan, "An experimental and simulation study of performance and emission of MDF fueled direct injection in high compression ignition engine," *Biofuels, Bioprod. Biorefining*, vol. 9, no. 5, pp. 581–594, Sep. 2015, DOI: 10.1002/bbb.1557.

[13] H. J. Kim, H. K. Suh, and C. S. Lee, "Numerical and Experimental Study on the Comparison between Diesel and Dimethyl Ether (DME) Spray Behaviors According to Combustion Chamber Shape," *Energy & Fuels*, vol. 22, no. 4, pp. 2851–2860, Jul. 2008, DOI: 10.1021/ef8000696.

[14] D. I. Diesel, T. Diesel-RK, and T. Diesel-RK, "Software for engine simulation and optimisation."
[15] J. A. Gatowski, E. N. Balles, K. M. Chun, F. E. Nelson, J. A. Ekchian, and J. B. Heywood, "Heat release analysis of engine pressure data," 1984.
[16] Z. Şahin and O. Durgun, "Theoretical investigation of effects of light fuel fumigation on diesel engine performance and emissions," *Energy Convers. Manag.*, vol. 48, no. 7, pp. 1952–1964, 2007, doi: 10.1016/j.enconman.2007.01.027.
[17] A. Alqahtani, F. Shokrollahihassanbarough, and M. Wyszynski, "Thermodynamic simulation comparison of AVL BOOST and Ricardo WAVE for HCCI and SI engines optimisation," *Combust. Engines*, vol. 161, no. 2, pp. 68–72, 2015.
[18] S. Ramachandran, "Rapid Thermodynamic Simulation Model of an Internal Combustion Engine on Alternate Fuels," *Proc. Int. MultiConference Eng. Comput. Sci.*, vol. 2, no. 7, pp. 2146–2151, 2009.
[19] V. V. Le, A. T. Hoang, S. Nižetić, and A. I. Ölçer, "Flame characteristics and ignition delay times of 2,5-dimethylfuran: A systematic review with comparative analysis," *J. Energy Resour. Technol. Trans. ASME*, vol. 143, no. 7, pp. 1–16, 2021, doi: 10.1115/1.4048673.
[20] A. S. Kuleshov, "Model for predicting air-fuel mixing, combustion and emissions in DI diesel engines over the whole operating range," *SAE Pap.*, no. 2005–01, p. 2119, 2005, DOI: 10.4271/2005-01-2119.
[21] M. M. Abou Al-Sood, M. Ahmed, and Y. M. Abdel-Rahim, "Rapid thermodynamic simulation model for optimum performance of a four-stroke, direct-injection, and variable-compression-ratio diesel engine," *Int. J. Energy Environ. Eng.*, vol. 3, no. 1, p. 13, 2012, DOI: 10.1186/2251-6832-3-13.
[22] B. K. Debnath, N. Sahoo, and U. K. Saha, "Thermodynamic analysis of a variable compression ratio diesel engine running with palm oil methyl ester," *Energy Convers. Manag.*, vol. 65, pp. 147–154, 2013, doi: 10.1016/j.enconman.2012.07.016.
[23] A. Kuleshov, K. Mahkamov, A. Kozlov, and Y. Fadeev, "Simulation of Dual-Fuel Diesel Combustion With Multi-Zone Fuel Spray Combustion Model," *Vol. 2 Instrumentation, Control. Hybrids; Numer. Simulation; Engine Des. Mech. Dev. Keynote Pap.*, p. V002T06A020, 2014, DOI: 10.1115/ICEF2014-5700.
[24] A. Khaliq, S. K. Trivedi, and I. Dincer, "Investigation of a wet MDF operated HCCI engine based on first and second law analyses," *Appl. Therm. Eng.*, vol. 31, no. 10, pp. 1621–1629, 2011, doi: 10.1016/j.applthermaleng.2011.02.001.
[25] B. Guan, R. Zhan, H. Lin, and Z. Huang, "Review of the state of the art technologies of selective catalytic reduction of NOx from diesel engine exhaust," *Appl. Therm. Eng.*, vol. 66, no. 1–2, pp. 395–414, 2014, doi: 10.1016/j.applthermaleng.2014.02.021.
[26] A. S. Kuleshov, A. V Kozlov, and K. Mahkamov, "Self-Ignition delay Prediction in PCCI direct injection diesel engines using multi-zone spray combustion model and detailed chemistry," 2010.
[27] A. Fayyazbakhsh and V. Pirouzfar, "Comprehensive overview on diesel additives to reduce emissions, enhance fuel properties and improve engine performance," *Renew. Sustain. Energy Rev.*, vol. 74, pp. 891–901, 2017, doi: 10.1016/j.rser.2017.03.046.
[28] D. D. Wickman, P. K. Senecal, and R. D. Reitz, "0," 2001, DOI: 10.4271/2001-01-0547.
[29] J. Benajes, S. Molina, R. Novella, and K. DeRidder, "Influence of injection conditions and exhaust gas recirculation in a high-speed direct-injection diesel engine operating with a late split injection," *Proc. Inst. Mech. Eng. Part D J. Automob. Eng.*, vol. 222, no. 4, pp. 629–641, 2008, doi: 10.1243/09544070JAUTO657.
[30] D. C. Rakopoulos, C. D. Rakopoulos, R. G. Papagiannakis, and D. C. Kyritsis, "Combustion heat release analysis of ethanol or n -butanol diesel fuel blends in heavy-

 https://doi.org/10.37896/pd91.3/91329

duty DI diesel engine," *Fuel*, vol. 90, no. 5, pp. 1855–1867, 2011, doi: 10.1016/j.fuel.2010.12.003.

[31] U. Asad and M. Zheng, "Fast heat release characterisation of a diesel engine," *Int. J. Therm. Sci.*, vol. 47, no. 12, pp. 1688–1700, 2008, doi: 10.1016/j.ijthermalsci.2008.01.009.

[32] V. Hariram and R. Vagesh Shangar, "Influence of compression ratio on combustion and performance characteristics of direct injection compression ignition engine," *Alexandria Eng. J.*, vol. 54, no. 4, pp. 807–814, 2015, doi: 10.1016/j.aej.2015.06.007.

[33] L. Xing-Cai, Y. Jian-Guang, Z. Wu-Gao, and H. Zhen, "Effect of cetane number improver on heat release rate and emissions of a high-speed diesel engine fueled with MDF-diesel blend fuel," *Fuel*, vol. 83, no. 14-15 SPEC. ISS., pp. 2013–2020, 2004, doi: 10.1016/j.fuel.2004.05.003.

[34] W. Tutak, A. Jamrozik, M. Pyrc, and M. Sobiepański, "Investigation on the combustion process and emissions characteristic in direct injection diesel engine powered by wet MDF using blend mode," *Fuel Process. Technol.*, vol. 149, pp. 86–95, 2016, doi: 10.1016/j.fuproc.2016.04.009.